

# Evaluating Mechanical Properties of CoNiCrAlY Coating from Miniature Specimen Testing at Elevated Temperature

W. Wen, G. Jackson, S. Maskill, D. G. McCartney, W. Sun

**Abstract**—CoNiCrAlY alloys have been widely used as bond coats for thermal barrier coating (TBC) systems because of low cost, improved control of composition, and the feasibility to tailor the coatings microstructures. Coatings are in general very thin structures, and therefore it is impossible to characterize the mechanical responses of the materials via conventional mechanical testing methods. Due to this reason, miniature specimen testing methods, such as the small punch test technique, have been developed. This paper presents some of the recent research in evaluating the mechanical properties of the CoNiCrAlY coatings at room and high temperatures, through the use of small punch testing and the developed miniature specimen tensile testing, applicable to a range of temperature, to investigate the elastic-plastic and creep behavior as well as ductile-brittle transition temperature (DBTT) behavior. An inverse procedure was developed to derive the mechanical properties from such tests for the coating materials. A two-layer specimen test method is also described. The key findings include: 1) the temperature-dependent coating properties can be accurately determined by the miniature tensile testing within a wide range of temperature; 2) consistent DBTTs can be identified by both the SPT and miniature tensile tests (~ 650 °C); and 3) the FE SPT modelling has shown good capability of simulating the early local cracking. In general, the temperature-dependent material behaviors of the CoNiCrAlY coating has been effectively characterized using miniature specimen testing and inverse method.

**Keywords**—CoNiCrAlY coatings, mechanical properties, DBTT, miniature specimen testing.

## I. INTRODUCTION

CoNiCrAlY coatings have been widely used as the bond coatings for TBC systems, due to the relatively low cost, improved control of composition, and the feasibility to customize and design the microstructures [1], [2]. The bond coatings (a critical part of a TBC system) require very good understanding of the material performance. However, the focus of most previous studies has been on the oxidation behavior and the availability of the mechanical properties is very limited [3]-[5]. Therefore, a more comprehensive mechanical characterization of coating materials is highly valuable. The investigation on the free-standing bond coatings is also an important necessary step to the characterization of the two-material or multi-material systems, such as the TBC systems.

W. Wen is a PhD researcher in the Department of Mechanical, Materials and Manufacturing Engineering at University of Nottingham (e-mail: wu.wen@nottingham.ac.uk).

G. A. Jackson is a Research Fellow, S. Maskill is a Senior Engineer, D. G. McCartney is a Professor, and W. Sun is a Professor in the Department of Mechanical, Materials and Manufacturing Engineering at University of Nottingham.

For example, before carrying out investigation on a TBC system, it would be necessary to study the material behaviors of the substrate material, the bond coating and the TBC, separately.

Investigations into the mechanical properties of CoNiCrAlY coatings have been carried out using a variety of experimental techniques (e.g. 4-point bending, local indentation) [6], [7], but there is still little consistent data for any single CoNiCrAlY coating. Recently, studies have employed the small punch tensile (SPT) test to determine the mechanical properties and DBTT of CoNiCrAlY coatings [8]-[10]. The SPT test is suitable for coatings as it employs small specimens: 8 mm diameter discs of 0.5-mm thickness. The SPT test has been widely applied as an effective method to determine the mechanical properties and DBTT of steels [11], [12], and the recent studies have demonstrated the applicability of the SPT test for CoNiCrAlY coatings.

Efforts have also been made by researchers to develop miniaturized tensile testing (e.g. [13], [14]). Most of those studies are carried out on typical metal alloys, but few applications have been extended to coatings. For the sprayed coatings, the presence of porosity is generally expected, though it can be reduced by heat treatments [10], [15]. Due to the miniaturized size of the specimen, the local heterogeneity induced by the existence of porosity could have non-negligible influences on the testing results and may lead to significant scatters of the test data. Similarly, the effects of surface oxidation might also be amplified by the miniaturized size of the specimens.

Inverse methods have been employed in many studies to characterize material behaviors based on the data obtained from various testing techniques, such as micro-indentation tests (e.g. [16], [17]), three-point bending tests (e.g. [18]), and SPT tests (e.g. [19], [20]). One of the advantages of inverse methods is that it can produce relatively accurate properties quickly. In principle, most of factors of influence can be taken into considerations by inverse methods since they are entirely based on the experimentally measurable quantities. However, it also means that the validity of inverse methods greatly depends on the accuracy and consistency of the physical experimental data. It should be noted that inverse methods could incur high computation cost, especially when complex finite element (FE) analysis is involved.

This paper presents an overview on some recent studies on assessing the elastic-plastic behavior of a CoNiCrAlY coating at room and high temperatures, through the use of the small

punch testing and the newly developed miniature specimen tensile testing, to evaluate the elastic-plastic (and creep) behavior, DBTT behavior, and to derive the mechanical properties from such tests for the coating material through the use of inverse methods. A two-layer specimen test method is also introduced. Limitation of the current methods and future improvement are discussed.

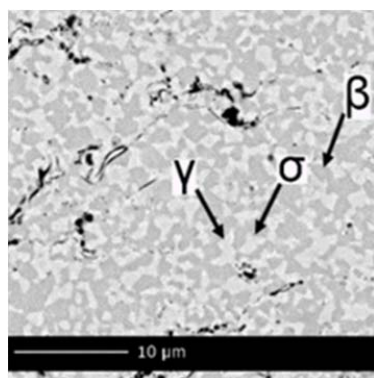
## II. MATERIAL AND EXPERIMENTAL TESTING

### A. CoNiCrAlY Bond Coatings

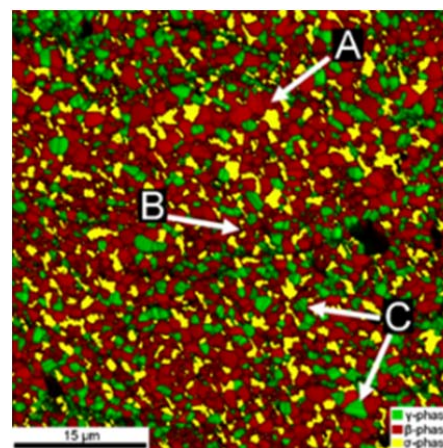
The CoNiCrAlY coating was prepared by HVOF thermal spraying using powders with the following nominal composition: Ni-20Co-22.3Cr-12.2Al-0.3Y. The phase fractions in volume percentage for the coating are listed in Table I [11]. Vacuum heat treatment was carried out on free-standing samples at 1100 °C for two hours in an Elite Thermal Systems TVH12 vacuum tube furnace held at approximately 10<sup>-9</sup> bar followed by furnace cooling to room temperature for 6 hours. This treatment was applied in order to approximately replicate the initial heat treatment given to bond coats during the manufacture of TBC. This type of heat treatment has been shown to reduce the porosity commonly present within sprayed coatings and allows the precipitation of secondary phases [9], [10], [21]. The BSE image and the EBSD map of the untested coating after heat treatment are shown in Figs. 1 (a) and (b), respectively. The light contrast phase is an FCC Ni- $\gamma$ -phase and the dark contrast phase is a BCC NiAl- $\beta$ -phase. The dark regions are Al<sub>2</sub>O<sub>3</sub> oxides. The letters A and B indicate areas of large and fine grains, respectively. The letter C indicates twinning in the  $\gamma$ -Ni phase. Specimens for SPT and miniature tensile tests were cut from the heat-treated coating by electro-discharge machining. They were grounded down from the as-deposited thickness to a final thickness of 400 and 500  $\mu$ m, respectively, on 1200 grade silicon carbide paper. The final thickness was controlled to within  $\pm 5$   $\mu$ m as measured by a digital micrometer, and both surfaces had the same finely ground surface finish.

TABLE I  
PHASE FRACTIONS (VOL.%) OF THE CONICRALY COATING

$\beta$ -NiAl	$\gamma$ -Ni	$\sigma$ -Cr <sub>2</sub> Co
60 $\pm$ 2	27 $\pm$ 2	13 $\pm$ 2



(a)



(b)

Fig. 1 (a) BSE image of the heat treated CoNiCrAlY coating and (b) EBSD scans of coating presented as a phase map [11]

### B. Small Punch Tensile Testing

Displacement controlled small punch tests were carried out at a displacement rate of  $1 \times 10^{-6}$  ms<sup>-1</sup> at room temperature (RT) and between 500-750 °C on a custom-built rig installed on a Tinius Olsen H5KS single column material testing machine. The temperature range was chosen to achieve brittle failure at the lower temperature and ductile failure at the higher temperature. A schematic of the small punch rig is shown in Fig. 2, where  $a_p=2$  mm,  $R_s=1.25$  mm and  $t_0=0.4$  mm are the radius of the receiving hole, punch head radius and specimen thickness, respectively. Full details on the small punch rig can be found in [10]. A three tier, 3 kW furnace was used to heat the specimens. Three K-type thermocouples, accurate to 5 °C, were used to measure the furnace temperature in the top, middle and bottom tiers. All tests were carried out in accordance with the CEN workshop agreement [21] in a temperature-controlled room held at 21 °C. The load was applied through a 2.5 kN load cell and the punch head displacement was measured by two LVDT's.

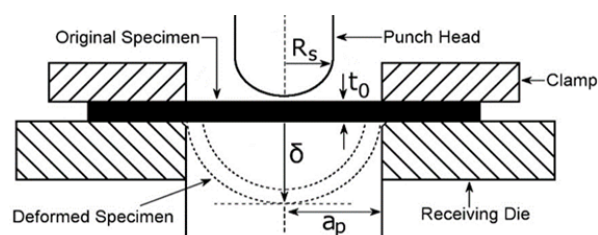


Fig. 2 Schematic cross section of the small punch rig

### C. Miniature Tensile Testing

The geometry and dimensions of the miniature tensile specimen are shown in Fig. 3 (a). Fig. 3 (b) shows the schematic of the loading assembly and how the miniature specimen was clamped and mounted to the machine [22]. The loading assembly parts were made of a high temperature nickel-based superalloy, Nimonic 115. The specimen was clamped at both ends by specially manufactured clamps with machined surface features to increase the friction between the

clamp and specimen. The displacement was measured by two LVDT's connected to both sides of the loading parts of the machine. The mounted specimens were heated in a 3 tier, 3 kW furnace except for the RT test. Tensile tests were carried out at RT, 500 °C, 600 °C, and 700 °C. Multiple tests were carried out at each temperature to verify the consistency of the testing method. The loading process was controlled at the constant displacement rate of 0.006 mm/s (to achieve a strain rate of 0.001/s, approximately). It had been verified by preliminary tests that the results of the tensile tests had very low sensitivity to the loading rate between 0.0006 mm/s and 0.06 mm/s. The torque applied to the clamps was adjusted to 0.5 Nm in order to avoid inducing any cracking in the specimen while providing sufficient clamping force to avoid slipping.

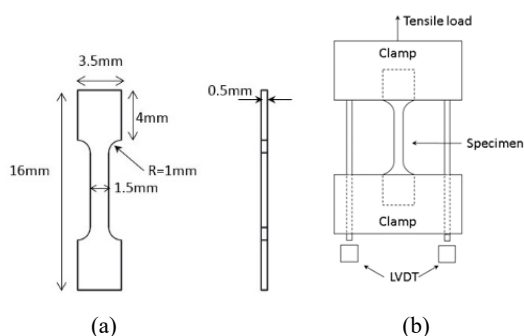


Fig. 3 Schematics of (a) the miniature tensile specimen and (b) the miniature tensile testing rig

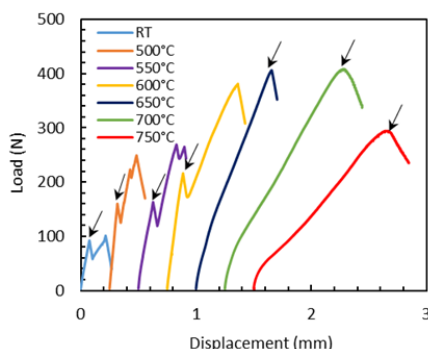


Fig. 4 Load-displacement curves of SPT tests on the CoNiCrAlY coating [11]

### III. MECHANICAL BEHAVIOR AND CHARACTERIZATION

#### A. Small Punch Tensile Testing

Representative load-displacement plots are shown in Fig. 4 following SPT tests at room temperature (RT) and between 500 and 750°C for the CoNiCrAlY coating (the load-displacement curves are plotted with displacement offset for clear view). There is a distinct change in the load-displacement behavior for the coatings as the temperature is increased. At high temperatures (700 and 750 °C), the curves are similar to those reported elsewhere for ductile materials [12], [22], [23] and display an initial linear region of elastic behavior followed by plastic deformation, membrane stretching, maximum load and then progressive plastic instability. Failure occurs shortly after

the maximum load, as has been observed for steels. At the lower temperatures, below 600 °C, the curves are predominately linear and feature sharp load drops which have been shown to indicate local fracture in non-ductile materials [10], [24], [25]. Hence, the point of fracture, indicated by the arrows in Fig. 4, is taken at the first load drop or characteristic change in the slope of the curve that is not associated with one of the four bending regions described above.

#### B. Miniature Tensile Testing

The engineering stress-strain curves, estimated from the loading force, original cross-section area and loading direction displacement, obtained from the miniature tensile tests are shown in Fig. 5. It should be noted that the displacement measurements were taken at the clamped ends (outside the gauge length region) because it is very difficult to fit a gauge into the very limited space. Therefore, the measured displacement was different from the actual displacement of the gauge length area. An equivalent gauge length ( $EGL$ ),  $L_{EGL} = \beta L_o$  ( $\beta$  is a constant decided by the geometry of the specimen and the loading conditions, and  $L_o$  is the original uniform gauge length), was estimated based on finite element analyses, where  $\beta \approx 1.2$ . The repeatability of the multiple tests carried out at each temperature, RT, 500 °C, 600 °C, and 700 °C, was very good. It is clear that the ultimate tensile stress (UTS) decreases as temperature increases from RT to 700 °C. At and below 600 °C, there was only the elastic deformation phase and the strain-hardening phase, but no clear sign of material softening before failure, while there was a clear phase of material softening before reaching failure at 700 °C. The observed material softening at 700 °C might be due to the recrystallisation of the material at elevated temperature. A notable phenomenon observed in the SPT tests on the same material was the sudden load drop at low strains, which indicated the possible formation of early cracking at and below 600 °C (shown in Fig. 4). However, no sign of early cracking was found in the miniature tensile tests, indicating that it is an effective mechanical testing technique for this coating material at a wide range of temperature, despite the ductile-to-brittle transition of the material.

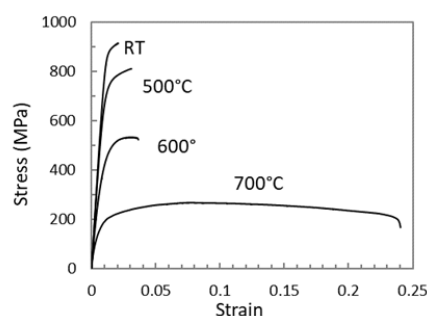


Fig. 5 Representative stress-strain curves converted from the miniature tensile tests of the CoNiCrAlY coating at different temperatures [26]

#### C. Ductile-Brittle Transition

The strain to first cracking as a function of temperature obtained from SPT tests is shown for both coatings in Fig. 6.

The empirical correlation (1) was used to estimate the strain at first cracking from the SPT testing results, where  $\delta$  is the displacement and  $t$  is the original specimen thickness. There is only a small increase in the strain at first cracking between RT and 600 °C, indicating that the ductility of the CoNiCrAlY coating does not change significantly over that temperature range. Between 600 and 700 °C, there is a large increase in the strain at first cracking which demonstrates there is a significant change in the ductility of the coating. Similar behaviors are found from the miniature specimen tensile tests between RT and 700 °C, as Fig. 7 shows the failure strain and UTS as functions of temperature.

$$\epsilon = 0.15 \left(\frac{\delta}{t}\right)^{1.5} \quad (1)$$

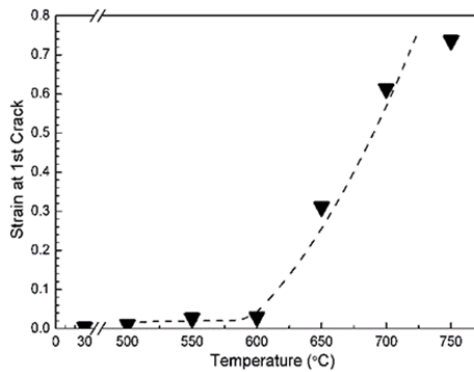


Fig. 6 The strain to first cracking as a function of temperature obtained from the SPT tests [11]

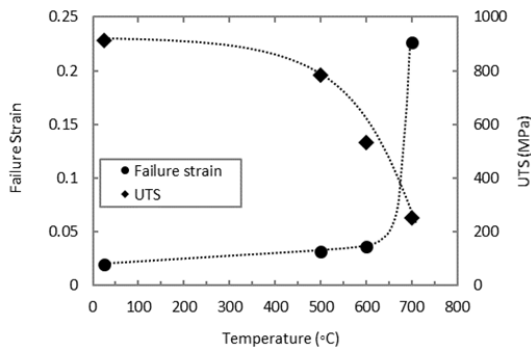


Fig. 7 The failure strain and UTS as a function of temperature obtained from the miniature specimen tensile tests [26]

Figs. 8 (a) and (b) show the fracture surfaces of the SPT specimens following the tests at 500 °C and 700 °C, respectively. The fracture at 500 °C was characterized by a star-like cracking pattern in the center of the specimen, as shown in Fig. 8 (a), known to be associated with brittle failure [26], [27]. At 700 °C, fracture was characterized by circumferential cracking, as seen in Fig. 8 (b), which is known to be associated with ductile failure [16], [24], [27]. These findings indicated that the DBTT of the coating was between 500-700 °C, in agreement with that reported in [10].

Secondary electron (SEM) images for the fracture surfaces of the miniature tensile tests specimens tested at 500 °C and

700 °C are shown in Figs. 9 (a) and (b), respectively. The scans were performed at high magnification because there was no significant difference in the macro-geometries of the specimens following the tests at different temperatures. At 500 °C, there are noticeable concave or convex features, which are relatively smooth and approximately up to 30 to 40 μm in size. These features are identified as powder particles which indicates brittle failure occurred along the powder particle boundaries. In contrast, no such features are identified on the fracture surface of the specimen tested at 700 °C. The 700 °C fracture surface consists of small, rounded surface features that indicate ductile failure.

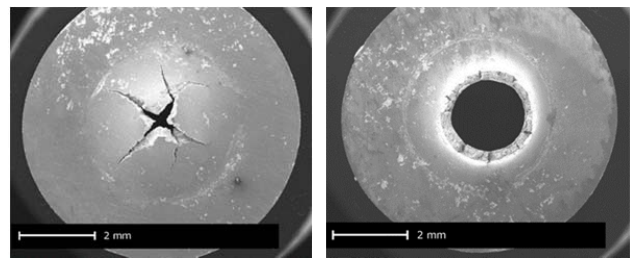


Fig. 8 Fracture surfaces of the SPT specimens of the CoNiCrAlY coating at (a) 500 °C and (b) 700 °C [26]

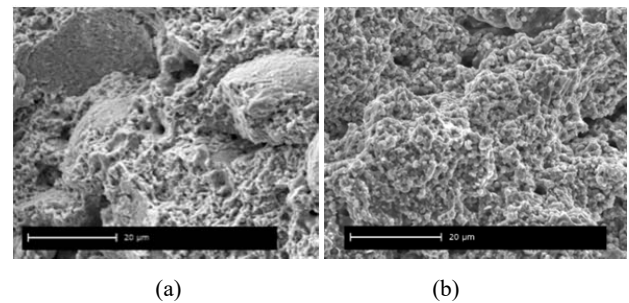


Fig. 9 SEM images of the fracture surfaces of the miniature tensile specimens of the CoNiCrAlY coating at (a) 500 °C and (b) 700 °C [26]

#### IV. INVERSE METHOD

##### A. Material Constitutive Model

To characterize the mechanical behaviors of the coating material, a simple Hooke's law was applied for the elastic deformation, i.e.  $\sigma = E\epsilon$ , where  $\sigma$  is the stress,  $\epsilon$  is the strain and  $E$  is the elastic modulus. For the plastic deformation, the Johnson-Cook constitutive model [28] was used to describe the strain hardening behavior, taking into account of the effects of temperature. The original Johnson-Cook model is expressed as:

$$\sigma = (A + B\epsilon^n)(1 + C \ln \dot{\epsilon}^*)(1 - T^{*m}) \quad (2)$$

$$\dot{\epsilon}^* = \frac{\dot{\epsilon}}{\dot{\epsilon}_0} \quad (3)$$

$$T^* = \frac{T - T_r}{T_m - T_r} \quad (4)$$

where  $A$  is the yield stress at the selected reference temperature,

$T_r$ ,  $B$  is the strain hardening coefficient,  $n$  is the strain hardening exponent,  $C$  is the material constant for strain rate hardening,  $m$  is the material constant for thermal softening exponent,  $\dot{\epsilon}$  is the applied strain rate,  $\dot{\epsilon}_0$  is the reference strain rate,  $T$  is the applied temperature and  $T_m$  is the melting temperature of the material (temperatures are in unit of K). The melting temperature of the CoNiCrAlY coating material is approximately 1350 °C or 1623 K (the powder used to prepare the coating was obtained from Praxair, powder code CO-210-24). In this study, the strain rate hardening was neglected. The Johnson-Cook constitutive equation, (1), was simplified as:

$$\sigma = (A + B\epsilon^n)(1 - T^{*m}) \quad (5)$$

It should be noted that the temperature effects on elastic properties are not included by the Johnson-Cook constitutive model.

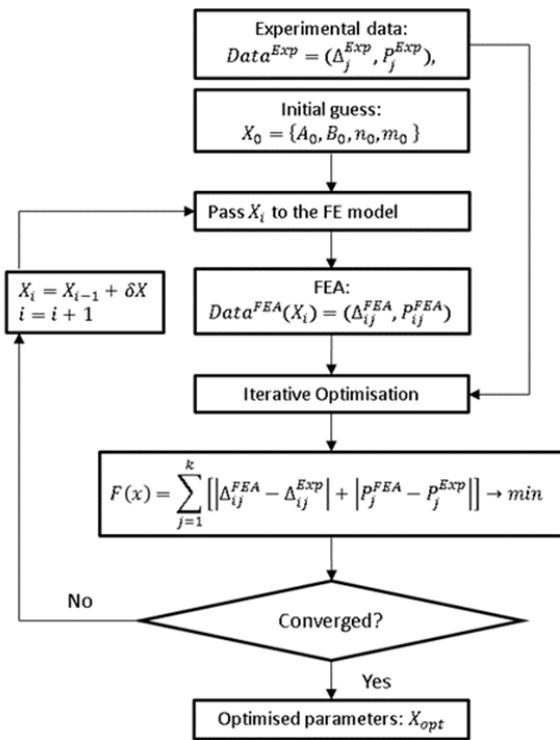


Fig. 10 Flowchart of the inverse method

### B. Inverse Method Procedures

An inverse method was developed to extract the Johnson-Cook constitutive properties from the miniature tensile tests on the CoNiCrAlY coating. Fig. 10 shows the flowchart of the inverse method. The experimental data obtained from the miniature tensile tests are supplied as the target values in the form of load ( $P$ )-displacement ( $\Delta$ ) curves. An initial guess of the Johnson-Cook constitutive properties is provided to start the iterative algorithm. This initial guess can be obtained by performing a numerical function fitting based on the Johnson-Cook constitutive equations and the stress-strain data obtained from a similar material. A nonlinear optimization function (fminsearch) within the optimization toolbox in the commercial

code MATLAB R2015a [29] was employed, cooperated with FE model of the miniature specimen, to obtain FE predictions for the corresponding miniature tensile tests and calculate the total differences compared to the experimental data. The FE results were extracted using a Python script constructed for the FE model built using the commercial code ABAQUS 6.14-1. An objective function was constructed to obtain the minimum value of the total differences between FE predictions and experimental results. The inverse algorithm stops automatically once the objective function value is minimized to be smaller than a user-defined threshold value. It should be noted that the constitutive constants ( $A$ ,  $B$ ,  $n$  and  $m$ ) are in very different orders. These constants need to be scaled to similar orders, based on a selected minimum step size, to ensure that the optimization algorithm works efficiently on all constitutive constants. The ratio of the minimum step size ( $5 \times 10^{-5}$ ) to the magnitude of the scaled constant ( $1 \times 10^{-3}$ ) is crucial, e.g. if the step size is too small then the optimization might not progress efficiently or might not able to converge to the target values. A selected number of data points were taken from each part of the load-displacement curve, i.e. more data points are taken from the curved part than the linear part (the Johnson-Cook constitutive model describes the plastic behaviors). Other constitutive material models, e.g. creep models and damage models, can also be conveniently adapted to this inverse approach with suitable adjustments.

### C. Inverse Method Application

The inverse approach was applied for the experimental load-displacement curves obtained from the miniature tensile tests. It should be noted that the shape of the experimental curves from 700 °C were very dissimilar to those from RT, 500 °C and 600 °C, e.g. the ductility was significantly higher with a long softening region. The Johnson-Cook constitutive model is more suitable for relatively small strain. Also, damage behavior was not included by this constitutive model. Therefore, the Johnson-Cook constitutive model was applied to the inverse method for the experimental data obtained at RT and 500 °C. According to (3), (4), it is clear that the constitutive properties are dependent on the choice of reference temperature. In this case, RT (293 K) was selected as the reference temperature, i.e. the constitutive constant  $A$  was the yield stress at RT.

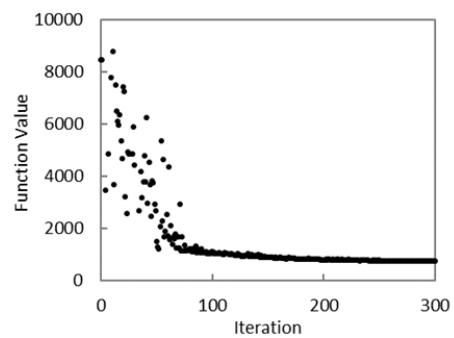


Fig. 11 Objective function evolution of the inverse approach [26]

The evolution of the optimization function is shown in Fig.

11. The function value is the measure of the total differences between the predicted load-displacement curves extracted from FE modelling and the experimental curves. It should be noted that the Johnson-Cook constitutive model does not take account of the temperature effects on the elastic modulus. The elastic modulus was taken as a constant for the optimization since it is relatively easy to extract the elastic modulus from the experimental results, but certain amount of error might still exist. The comparison between the target curves, initial guess and the optimized load-displacement curves is shown in Fig. 12. The optimized curves are much closer to the experimental curves than the initial guess. The initial guess and the optimized Johnson-Cook constitutive properties are summarized in Table II. Generally, the inverse method was proved to be capable of extracting the Johnson-Cook constitutive properties of the CoNiCrAlY coating using the miniature tensile testing results obtained at different temperatures with a very good agreement to the experimental data.

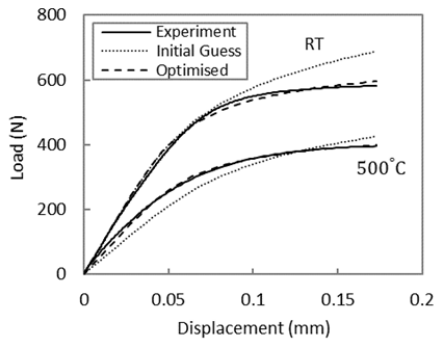


Fig. 12 Load-displacement curves: experiment, initial guess and optimized [26]

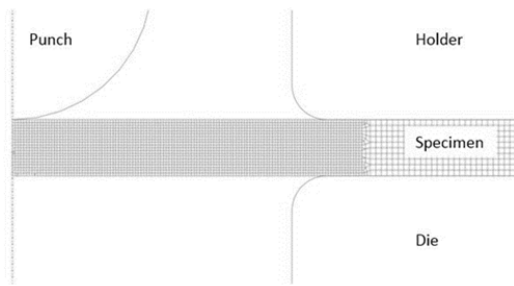


Fig. 13 The FE model of SPT Testing

TABLE II  
 THE INITIALLY ESTIMATED AND THE OPTIMIZED JOHNSON-COOK  
 CONSTITUTIVE PROPERTIES (RT AND 500°C) [26]

	A	B	n	m
Initial Estimation	700 MPa	1000	0.5	0.5
Optimized	765.16 MPa	607.18	0.3	1.715

### V. FINITE ELEMENT MODELLING

FE modelling of SPT tests of the CoNiCrAlY coating was carried out using the commercial code Abaqus with the stress-strain behavior acquired from the miniature specimen tensile tests. The geometry of the FE model was shown in Fig. 13 with

the identical dimensions for the SPT tests described in Section II. B. The punch head, the holder, and the die were modelled as axisymmetric analytical rigid bodies. The specimen was modelled as axisymmetric deformable body and meshed using the 4-node bilinear axisymmetric stress quadrilateral with reduced integration elements (CAX4R) and the 3-node linear axisymmetric stress triangle elements (CAX3) for the transition zones. Refined mesh with the elements size 0.02 mm was used for the un-supported region of the specimen due to the expected high stress and large deformation.

A failure mechanism was required to characterize the damage evolution of the SPT testing specimen. Fig. 14 shows a typical uniaxial stress-strain curve of a material with (a-b-c-d) and without (a-b-c-d') damage evolution. The ductile damage initiation criterion within ABAQUS [30] was used to predict the onset of the damage. This criterion is met if (6) is satisfied:

$$\omega_D \int \frac{\Delta \bar{\epsilon}_D^{pl}}{\bar{\epsilon}_D^{pl}} = 1 \quad (6)$$

where  $\omega_D$  is the state variable for damage initiation,  $\bar{\epsilon}_D^{pl}$  is the plastic strain at damage initiation which is a function of stress triaxiality and plastic strain rate, i.e.  $\bar{\epsilon}_D^{pl}(\eta, \dot{\epsilon}^{pl})$ , where  $\eta = -p/q$ , ( $p$  is the pressure stress, and  $q$  is the Mises equivalent stress). The incremental increase in the damage initiation state variable,  $\Delta\omega_D$ , is computed as

$$\Delta\omega_D = \int \frac{\Delta \bar{\epsilon}_D^{pl}}{\bar{\epsilon}_D^{pl}} \geq 0 \quad (7)$$

Damage evolution was predicted using a criterion based on the energy dissipated during the process [30]. The fracture energy per unit area,  $G_f$ , was estimated by calculating the integration of the stress-displacement curves obtained from the miniature specimen tensile tests and supplied to the damage evolution simulation with ABAQUS/Explicit. The increasing rate of the damage state variable,  $\dot{d}$ , is computed as

$$\dot{d} = \frac{L \dot{\bar{\epsilon}}^{pl}}{\bar{u}_f^{pl}} = \frac{\dot{u}^{pl}}{\bar{u}_f^{pl}} \quad (8)$$

where  $L$  is the characteristic length and  $\bar{u}_f^{pl}$  is the equivalent plastic displacement at failure and computed as

$$\bar{u}_f^{pl} = \frac{2G_f}{\sigma_{y0}} \quad (9)$$

where  $\sigma_{y0}$  is the yield stress at failure. When the maximum degradation is reached, e.g.  $d = 1$ , the element is regarded as failed and removed from the model by Abaqus [30]. As the tensile test proceeds, the global damage evolution is reflected by the increasing number of failed elements removed from the FE model.

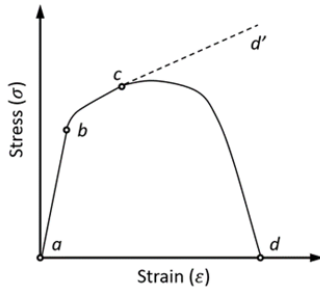


Fig. 14 A schematic representation of a uniaxial stress-strain curve with and without damage evolution [26]

The results of the FE modelling of SPT tests with and without damage evolution compared to the average experimental results are shown in Fig. 15. It should be noted that the Johnson-Cook properties presented in Table II were used for the FE modelling for RT and 500 °C while the estimated stress-strain data was used for 700 °C because the material became ductile at 700 °C and could not be accurately characterized using the Johnson-Cook model together with RT and 500 °C. At RT and 500 °C the maximum load tends to be overestimated when damage evolution is not included while it is predicted closer with damage evolution. More importantly, including damage evolution enables this FE model to predict the early load drops due to cracking found in the SPT tests at lower temperatures as the RT and 500 °C curves show.

The damage sites on the SPT specimen are depicted by the removal of the failed elements from the FE model. The comparison between the experimentally observed failure site for the 700 °C SPT testing specimen and the corresponding FE contour is shown in Fig. 16. The FE model was able to predict the failure site to be near the contact boundary of the specimen and the punch head. It should be noted that the current FE model was unable to predict the star-shaped brittle failure pattern observed at lower temperatures shown in Fig. 8 (a).

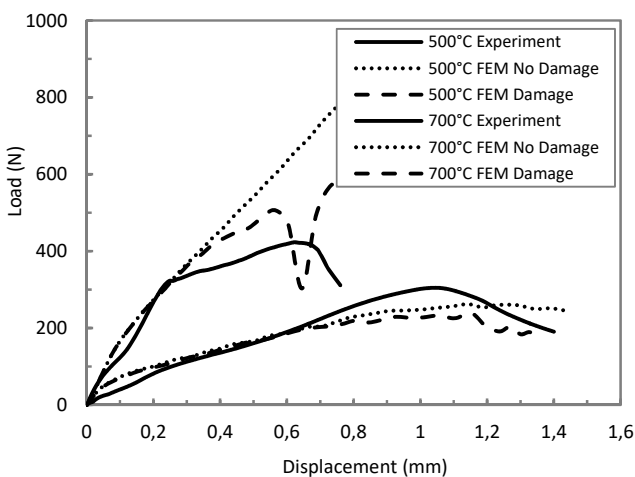


Fig. 15 The load-displacement curves: experimental data and FE modelling results of the SPT tests [26]

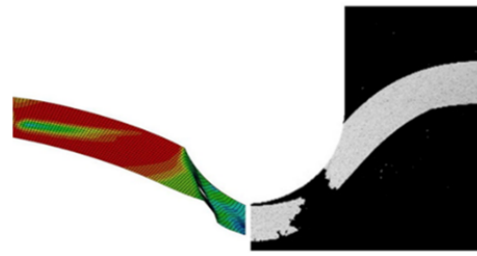


Fig. 16 The damage sites (a) predicted by FE modelling and (b) observed from the test for the 700 °C SPT test [11], [26]

## VI. CONCLUSIONS AND FUTURE WORK

### A. Conclusions

- The DBTT of the CoNiCrAlY coating has been found to occur at ~ 650 °C by both the SPT tests and the miniature specimen tensile tests, supported by the load-displacement or stress-strain data and the SEM images of the fracture surfaces following the SPT tests and the miniature specimen tensile tests.
- For SPT tests, fracture occurred at low strain and was characterized by cracking in the center of the specimen below the DBTT. Above the DBTT, circumferential cracking occurred at a radial offset from the center of the specimen at high strain.
- No early stage load drop has been found during the miniature specimen tensile tests.
- The inverse method developed has shown a good capability in determining the temperature-dependent mechanical properties of the coating from the miniature specimen tensile tests.
- The FE modelling of the SPT tests has shown to be able to produce comparable predictions with experimental results.

### B. Future Work

A two-material miniature tensile specimen shown in Fig. 17 is under the development by the authors. The two layers have equal length,  $L$ , equal width,  $d$ , and different thicknesses,  $h_1$  and  $h_2$ , therefore different cross-sectional areas,  $S_1$  and  $S_2$ . It is assumed that the properties of one of the materials are known in this case (e.g. the substrate material properties are known for a coated system). Since  $h_1$  and  $h_2$  are much smaller than  $L$ , it is assumed that the stresses in materials 1 and 2 in the uniform section are in a uniaxial state, i.e. the axial strains in the uniform section are identical. Tensile and creep tests can be conveniently carried out using such specimens.

The inverse method can be further extended and applied to determine the elastic-plastic and creep properties of the unknown material based on the experimentally obtained single-material specimen and two-material specimen compound behaviors.

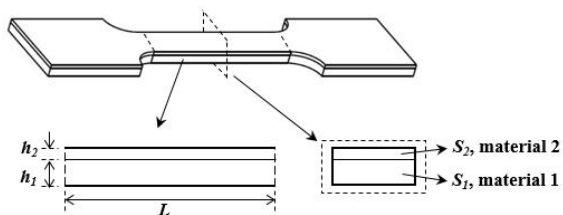


Fig. 17 Schematic of the miniature two-material specimen [31]

#### REFERENCES

[1] Lugsheider E, Herbst C, Zhao L. Parameter studies on high-velocity oxy-fuel spraying of MCrAlY coatings. *Surf. Coat. Technol.* 1998; 108-109:16–23.

[2] Higuera V, Belzunce FJ, Riba J. Influence of the thermal-spray procedure on the properties of a CoNiCrAlY coating. *Surf. Coat. Technol.* 2006; 200: 5550–5556.

[3] Chen H, Jackson GA, Sun W. An overview of using small punch testing for mechanical characterization of MCrAlY bond coats. *J. Therm. Spray Technol.* 2017; 26: 1222-1238.

[4] Tillmann W, Selvadurai U, Luo W. Measurement of the Young's modulus of thermal spray coatings by means of several methods. *J. Therm. Spray Technol.* 2013; 22: 290-298.

[5] Waki H, Oikawa A, Kato M, Takahashi S, Kojima Y, Ono F. Evaluation of the accuracy of Young's moduli of thermal barrier coatings determined on the basis of composite beam theory. *J. Therm. Spray Technol.* 2014; 23: 1291-1301.

[6] Itoh Y, Saitoh M. Mechanical properties of overaluminized MCrAlY coatings at room temperature. *J. Eng. Gas Turb. Power.* 2005; 127:807–813.

[7] Hemker KJ, Mendis BG, Eberl C. Characterizing the microstructure and mechanical behaviour of a two-phase NiCoCrAlY bond coat for thermal barrier systems. *Mat. Sci. Eng. A.* 2008; 483-484:77–730.

[8] Eskner M, Sandstrom R. Mechanical properties and temperature dependence of an air plasma-sprayed NiCoCrAlY bondcoat. *Surf. Coat. Technol.* 2006; 200(8): 2695 – 2703.

[9] Chen H, Hyde TH, Voisey KT, McCartney DG. Application of small punch creep testing to a thermally sprayed CoNiCrAlY bond coat. *Mater. Sci. Eng.: A.* 2013; 585:205–213.

[10] Jackson GA, Sun W, McCartney DG. The Application of the Small Punch Tensile Test to Evaluate the Ductile to Brittle Transition of a Thermally Sprayed CoNiCrAlY Coating. *Key Eng. Mater.* Vol. 2017; 734: 144-155.

[11] Jackson GA, Sun W, McCartney DG. The influence of microstructure on the ductile to brittle transition and fracture behaviour of HVOF NiCoCrAlY coatings via SP tensile testing. *Mater. Sci. Eng. A.* 2019; 754: 479-490.

[12] Mao X. Small punch test to predict ductile fracture toughness JIC and brittle fracture toughness KIC. *Scripta Metallurgica et Materialia.* 1991; 25:2481–2485.

[13] Cao L, Bürger D, Wollgramm P, Neuking K, Eggeler G. Testing of Ni-base superalloy single crystals with circular notched miniature tensile creep (CNMTC) specimens. *Mater. Sci. Eng. A.* 2018; 712: 223-231.

[14] Farrukh H, Desmukh MN, Husain Asif, Sehgal DK. Miniature test technique for acquiring true stress-strain curves for a large range of strains using a tensile test and inverse finite element method. *Applied Mech. Mater.* 2011; 110-116: 4204-4211.

[15] Kundan K, Arun P, Madhusoodanan K, Singh RN, Arnomitra C, Dutta BK., Sinha RK, Optimisation of thickness of miniature tensile specimens for evaluation of mechanical properties. *Mater. Sci. Eng. A.* 2016; 675: 32-43.

[16] Wen W, Becker AA, Sun W. Determination of material properties of thin films and coatings using indentation tests: a review. *J. Mater. Sci.* 2017; 52: 12553-12573.

[17] Kang JJ, Becker AA, Wen W, Sun W. Extracting elastic-plastic properties from experimental loading-unloading indentation curves using different optimization techniques. *Int. J. Mech. Sci.* 2018; 144: 102-109.

[18] Lu J, Campbell-Brown A, Tu Shan-Tung, Sun W. Determination of creep damage properties from miniature thin beam bending using an inverse approach. *Key Eng. Mater.* 2017; 734: 260-72.

[19] Husain Asif, Sehgal DK, Pandey RK. An inverse finite element procedure for the determination of constitutive tensile behaviour of materials using

miniature specimen. *Comput. Mats. Sci.* 2004; 31: 84-92.

[20] Saeidi S, Voisey KT, McCartney DG. The effect of heat treatment and the oxidation behaviour of HVOF and VPS CoNiCrAlY coatings. *J. Therm. Spray Technol.* 2009; 18: 209–216.

[21] CEN CWA 15627 Workshop Agreement: Small punch test method for metallic materials. European Committee for Standardization, Brussels, December 2006.

[22] Kameda J, Mao X. Small-punch and TEM-disc testing technique and their application to characterization of radiation damage. *J. Mater. Sci.* 1992; 27(4):983–989.

[23] Eskner M, Sandstrom R. Measurement of the ductile-to-brittle transition temperature in a nickel aluminide coating by a miniaturised disc bending test technique. *Surf. Coat. Technol.* 2003; 165(1):71 – 80.

[24] Lancaster RJ, Illsley HW, Davies GR, Jeffs SP, Baxter GJ. Modelling the small punch tensile behaviour of an aerospace alloy. *Mater. Sci. Technol.* 2017; 33 (9).

[25] Rasche S, Kuna M. Improved small punch testing and parameter identification of ductile to brittle materials. *Int. J. Pre. Ves. Pip.* 2015; 125: 23-34.

[26] Wen W, Jackson GA, Li H, Sun W. An experimental and numerical study of a CoNiCrAlY coating using miniature specimen testing techniques. *Int. J. Mech. Sci.* 2019; 157–158: 348-356.

[27] Ray AK. Failure mode of thermal barrier coatings for gas turbine vanes under bending. *Int. J. Turb. Jet.* 2000; 17: 1–24.

[28] Johnson GR, Cook WH. A constitutive model and data for metals subjected to large strains, high strain rates, and high temperatures. *Proc. 7th Int. Symp. on Ballistics, Hague, Netherlands, 1983 April.*

[29] Mathworks. *Global Optimization Toolbox: User's Guide (r2015a).* 2015.

[30] *Abaqus Analysis User's Manual.* (2009) Providence, RI: Simulia.

[31] Wen W, Sun W, Becker AA. Development of a two-material miniature specimen testing technique and the associated inverse approach. *Theor. Appl. Fract. Mech.* 2019; 99: 1-8.